10. L. S. Wang, H. S. Cheng, J. Fan, *J. Chem. Phys.* **102**, 9480 (1995).
11. L. S. Wang, H. Wu, in *Advances in Metal and Semiconductor Clusters. IV. Cluster Materials*, M. A. Duncan, Ed. (JAI Press, Greenwich, CT, 1998), pp. 299–343.
12. The $Li_3Al_4^-$ species were produced using a laser vaporization supersonic cluster source and an Al-Li alloy target. A wide range of $Li_xAl_y^-$ anionic clusters was produced and analyzed with a time-of-flight mass spectrometer. The $Li_3Al_4^-$ anions of interest were selected for photodetachment in each experiment. Photoelectron spectra were taken at two detachment laser wavelengths, 355 and 193 nm, and were calibrated using the known spectra of Cu^-. The photoelectron energy resolution was about 25 meV for 1-eV electrons.
13. We initially optimized geometries and calculated frequencies of $Li_3Al_4^-$ using analytical gradients with polarized split-valence basis sets (6-311+G*) and a hybrid method known in the literature as B3LYP. The energies of the most stable structures were refined using the coupled-cluster method with single, double, and noniterative triple excitations [CCSD(T)] and the most extended 6-311+G(2df) basis sets. The vertical electron detachment energies were calculated using the outer valence Green Function method [OVGF/6-311+G(2df)] and the B3LYP/6-311+G* geometries for $Li_3Al_4^-$. Core electrons were kept frozen in treating the electron correlations at the CCSD(T) and OVGF levels of theory. All calculations were performed using the Gaussian 98 program on a 63-nodes Birch-Retford Beowulf cluster computer built at Utah State by K. A. Birch and B. P. Retford.
14. M. J. Frisch *et al*., *Gaussian 98* (revision A.7), Gaussian Inc., Pittsburgh, PA (1998).
15. S. Chasko, M. Desphande, D. G. Kanhere, *Phys. Rev. B* **64**, 155409 (2001).
16. We did not observe much contribution from the triplet capped octahedron structure, whose first vertical detachment energy is rather low (Table 1). It may be that the triplet isomer is actually higher in energy than we estimated from our calculations. The expansion of one-electron basis sets and inclusion of higher orders in the coupled cluster theory usually increase stability of the singlet state over the corresponding triplet state.
17. The MO pictures were made with the MOLDEN3.4 program (G. Schaftenaar, MOLDEN3.4, CAOS/CAMM Center, Netherlands, 1998).
18. The calculated molecular properties of other low-lying isomers are given in tables S1 to S5.
19. The theoretical work done at Utah was supported by the donors of the Petroleum Research Fund, administered by the American Chemical Society. The experimental work done at Washington was supported by the National Science Foundation. The experiment was performed at the W. R. Wiley Environmental Molecular Sciences Laboratory, a national scientific user facility sponsored by the Office of Biological and Environmental Research of the U.S. Department of Energy (DOE) and located at Pacific Northwest National Laboratory, which is operated for DOE by Battelle.

Supporting Online Material

www.sciencemag.org/cgi/content/full/300/5619/622/DC1
Fig. S1
Tables S1 to S5

17 January 2003; accepted 17 March 2003

Casting Metal Nanowires Within Discrete Self-Assembled Peptide Nanotubes

Meital Reches and Ehud Gazit*

Tubular nanostructures are suggested to have a wide range of applications in nanotechnology. We report our observation of the self-assembly of a very short peptide, the Alzheimer's β-amyloid diphenylalanine structural motif, into discrete and stiff nanotubes. Reduction of ionic silver within the nanotubes, followed by enzymatic degradation of the peptide backbone, resulted in the production of discrete nanowires with a long persistence length. The same dipeptide building block, made of D-phenylalanine, resulted in the production of enzymatically stable nanotubes.

Self-assembled nanostructures provide a key direction for the controlled fabrication of novel nanoscopic materials and devices. Nanotubular structures are particularly important structural elements because they may serve as nanowires or nanoscaffolds (*1–4*). Peptide nanotubes are especially intriguing assemblies because they have the scope for numerous chemical modifications and allow the use of biological systems specificity. A milestone in the production of peptide-based nanotubes was the demonstration by Ghadiri *et al.* (*2*, *5*) that a cyclic octapeptide with alternating L and D amino acids can form a nanotubular structure by self-assembly. However, the peptide nanotubes that formed further assembled into an array of tubes that were aligned as crystalline microscopic structures (*2*, *5*). Linear surfactant-like hepta- and octapeptides can also self-assemble into a network of open-ended nanotubes, from which nanovesicles can "bud" or "fuse" (*3*, *4*). Peptide-related bis(*N*-α-amido-glycylglycine)-1,7-heptane dicarboxylate molecules were also shown to be assembled into tubular structures (*6*).

We observed the formation of peptide nanotubes while studying the ability of very short aromatic peptides (hexapeptides and shorter) to form well-ordered amyloid fibrils (*7–9*). Amyloid fibrils are the hallmark of a diverse group of diseases of unrelated origin, including Alzheimer's disease, type II diabetes, and prion diseases (*10–15*). Despite their formation by a diverse and structurally unrelated group of proteins, all amyloid fibrils share similar biophysical and structural properties. On the basis of both experiments and theory, we recently suggested that stacking of aromatic residues may play a key role in the process of molecular recognition and self-assembly that leads to the formation of amyloid fibrils (*16*). This proposal is in agreement with the well-known role of aromatic stacking in the formation of chemical and biochemical supramolecular structures (*17–19*). According to our suggestion, the restricted geometry and the attractive forces of the aromatic moieties provide order and directionality as well as the energetic contribution needed for the formation of such well-ordered structures. In this context, we were intrigued to determine the molecular properties of a peptide fragment corresponding to the core recognition motif of Aβ, the diphenylalanine element (Fig. 1A). This motif is of special interest, because several studies have identified the ability of larger peptides and conjugated organic molecules that contain this motif to inhibit fibril formation by Aβ (*20–22*). Some of those inhibitors are currently undergoing clinical trials as potential drugs to treat Alzheimer's disease (*23*, *24*).

Here, we sought to make the NH_2-Phe-Phe-COOH dipeptide soluble at very high concentrations (≥100 mg/ml) by dissolving the lyophilized peptide in 1,1,1,3,3,3 hexafluoro-2-propanol. Although the peptide appeared to be highly soluble in the organic solvent, a rapid assembly into ordered semi-crystalline structures was observed visually within seconds after dilution into the aqueous solution at a final μM concentration range. We used dynamic light scattering analysis to determine assembly into supramolecular structures within minutes at the μM range. Transmission electron microscopy (TEM) analysis with negative staining indicated that the peptide forms well-ordered, tubular, and elongated assemblies (Fig. 1B). The light shell and the dark center, as observed in Fig. 1B, suggested hollow tubular structures filled with the negative stain, uranyl acetate. Energy-dispersive x-ray analysis (EDX) indicated the presence of uranium within the assembled structures (fig. S1A). Smaller structures could also be observed by TEM analysis; we propose that these represent smaller tubular assemblies or fragments of the larger nanotubes. The persistence length of the nanotubes appears to be on the order of microme-

Department of Molecular Microbiology and Biotechnology, George S. Wise Faculty of Life Sciences, Tel Aviv University, Tel Aviv 69978, Israel.

*To whom correspondence should be addressed. E-mail: ehudg@post.tau.ac.il

ters, as evident by the microscopic observation. The formation of the tubular structures was very efficient. Almost all the assemblies as observed by TEM had tubular structures, and almost no amorphous aggregates were observed (<1%). This observation is in marked contrast to other peptide assemblies (such as amyloid fibrils) in which a mixture of ordered and aggregated structures may be observed. High-resolution field emission gun TEM (HR-TEM) (Fig. 1C) provided further indication of the regular structures of the tube walls. The formed structures were highly ordered and appeared to be rather stiff but without the usual branching and curving typical of amyloid fibrils. On the other hand, the assemblies show some morphological similarity in terms of size and tubular structures to the recently observed peptide nanotubes that are formed by much longer surfactant-like hepta- to octapeptides (*3*). These structures are different from the first-reported peptide nanotubes that were formed by cyclic polypeptides made of alternating D and L amino acids (*5*).

We used scanning electron microscopy (SEM) to further study the tubular structures (Fig. 2, A and B). The nanotubes were applied on a glass coverslip coated with gold and imaged by SEM. The low-magnification micrographs of areas filled with individual nanotubes (Fig. 2A) further demonstrate that the tubes are relatively homogeneous and evidently are individual entities with a persistence length on the order of micrometers. Figure 2C shows the statistical distribution of the diameters of the nanotubes. The crystal structure of the diphenylalanine peptide, as formed by evaporation of aqueous solution at 80°C, showed a crystal packing of aligned and elongated long hollows (*25*). These structures are also referred to as peptide nanotubes. However, our structural analysis indicates that the crystal packing of the peptide represents a completely different molecular arrangement compared with the self-assembled individual tubular structures. Higher magnification SEM analysis also indicated a typical nanotubular structure that resembled, to some extent, a class of peptide nanotubes that were recently reported (*3*), although our structures are apparently stiffer and discrete (Fig. 2B).

To gain insight into the molecular configuration of the assembled structures, we used Fourier-transformed infrared spectroscopy (fig. S2). Spectral analysis of the assemblies showed a sharp 1630 cm^{-1} peak at the amide I region. This peak is consistent with a β sheet–like conformation of the single amide bond, as was suggested for peptide nanotubes built of larger building blocks (*1*–*4*) and for amyloid fibrils (*9*). Because the dipeptide contains only a single amide bond, the vibrational assignment of this peak is definitive and does not represent an averaged contribution of several bonds, as occurs when longer peptide assemblies are analyzed. Moreover, no other vibrational peaks are observed (such as random coil peak around 1654 cm^{-1}) (*26*), which further suggests a uniform conformation of all the building blocks.

The formation of peptide nanotubes by the dipeptide is very interesting when viewed in the context of the mechanism of amyloid formation. Max Perutz recently suggested that amyloid fibers are water-filled nanotubes (*27*). The tubular structures formed by the dipeptides show a green-gold birefringence upon staining with Congo red dye, which is consistent with an organization that may be similar to that of amyloid structures. Therefore, it indicates that the extremely small core recognition motif of the β-amyloid polypeptide contains all the molecular information needed to mediate self-assembly into regular structures. The context in which the diphenylalanine recognition motif is set apparently dictates its assembly either into canonical amyloid fibrils, as is the case of Aβ, or into stiff nanotubes, as described here.

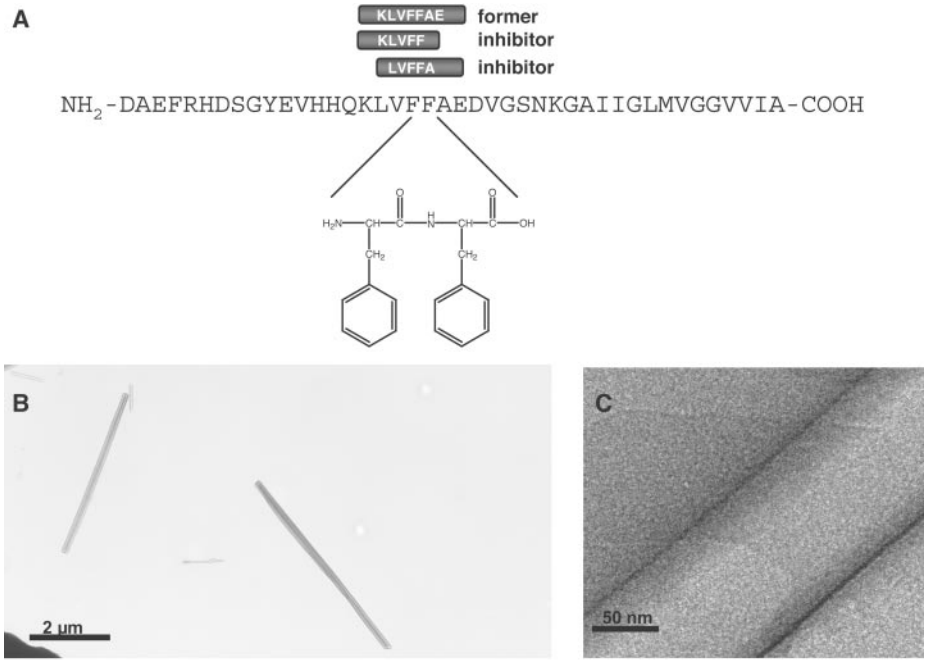

Fig. 1. Self-assembly of well-ordered and elongated peptide nanotubes by a molecular recognition motif derived from the β-amyloid polypeptide. (**A**) The central aromatic core of the β-amyloid polypeptide is involved in the molecular recognition process that leads to the formation of amyloid fibrils. Various fragments of the core form amyloid fibrils or inhibit their formation. (**B**) TEM images of the negatively stained nanotubes formed by the diphenylalanine peptide. (**C**) HR-TEM images of negatively stained peptide nanotubes, visualized by field emission gun microscope.

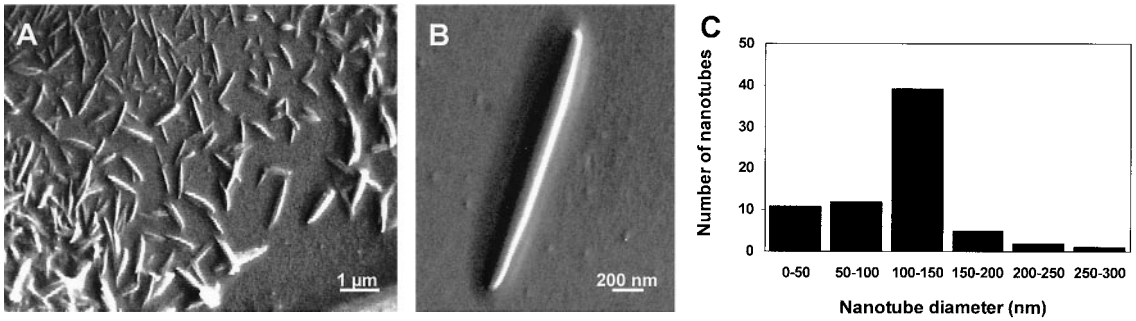

Fig. 2. Structural analysis of the tubular nanoparticles. (**A**) Low-magnification SEM images of a field of discrete nanotubes that are present as individual entities. (**B**) High-magnification SEM image of an individual nanotube. (**C**) A statistical distribution of nanotube diameters.

To study whether the tubes are indeed hollow and filled with aqueous solution, we added ionic silver to the nanotubes in solution. HR-TEM visualization followed by EDX analysis indicated that silver nanoparticles were formed within the tubes (fig. S1B). On the basis of these observations, we examined the ability of the nanotubes to serve as molds for casting metal nanowires (Fig. 3A). The tubes were added to boiling ionic silver solution, and the silver was reduced with citric acid to ensure a more uniform assembly of the silver nanowires (*28*, *29*). TEM analysis (without staining) indicated the formation of metal assemblies within the majority (80 to 90%) of the tubes (Fig. 3B). Proteolytic lysis of the peptide mold, by the addition of a proteinase K enzyme to the silver-filled nanotubes solution, resulted in the attainment of individual silver nanowires ~20 nm in diameter as seen by TEM (Fig. 3, C and D). The diameter of the nanowires is smaller than that of the tubes, which further suggests that casting was done inside the tubular structure. The chemical identity of the wire was confirmed by EDX analysis (fig. S1C).

For other applications, such as the assembly of nanotube-based biosensors or hollow tubing of nanofluidic circuits, enzymatically stable nanotubes are desirable. To assemble such stable tubes, we used proteolitically stable building blocks based on the D–amino acid analog of the peptide, NH_2-D-Phe-D-Phe-COOH. This peptide formed nanotubes with the same structural features as the corresponding L–amino acid peptide (Fig. 4A). After 1 hour of incubation of the Phe-Phe peptide with proteinase K (0.02 mg/ml), no tubular structures were observed by electron microscopy examination (as compared with hundreds of tubular structures observed before the proteolysis). In marked contrast, no notable variation could be observed before and after the incubation of the D-Phe-D-Phe peptide with the enzyme.

In light of the formation of nanotubes by such short dipeptides, we tested the ability of other aromatic dipeptides (Phe-Trp, Trp-Tyr, Trp-Phe, and Trp-Trp) under similar conditions. Nanoscale tubular structures were observed only in the case of the Phe-Trp peptide (Fig. 4B). However, substantial amounts of amorphous aggregates were also observed. This result differs markedly from the case of the Phe-Phe peptide, in which tubular structures were primarily observed.

Our studies present the synthesis of peptide nanotubes that are separated, are homogeneous, and have a long persistence length. The unique properties of the tubes and their proteolytic lability allow their use as nanoscale molds for the casting of silver nanowires. For other applications, enzymatically stable tubes can be fabricated.

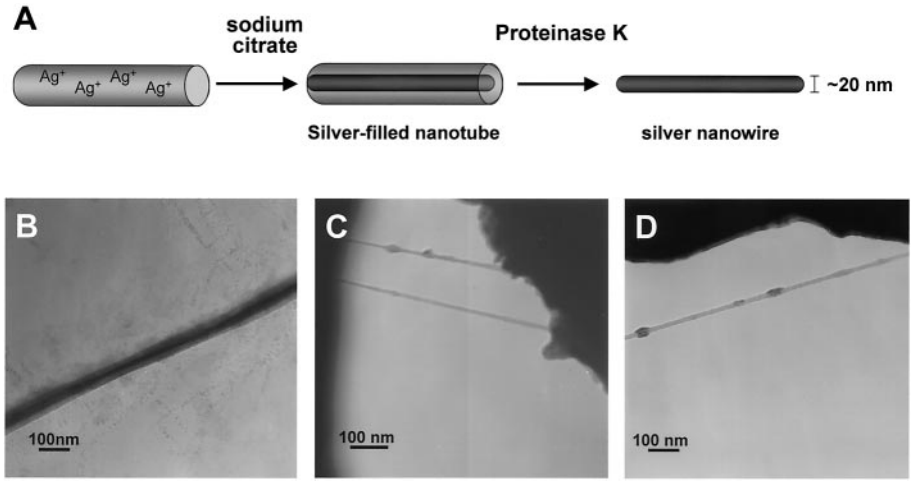

Fig. 3. Casting of silver nanowires with the peptide nanotubes. (**A**) The nanowires were formed by the reduction of silver ions within the tubes, followed by enzymatic degradation of the peptide mold. (**B**) TEM analysis (without staining) of peptide tubes filled with silver nanowires. (**C** and **D**) TEM images of silver nanowires that were obtained after the addition of the proteinase K enzyme to the nanotube solution.

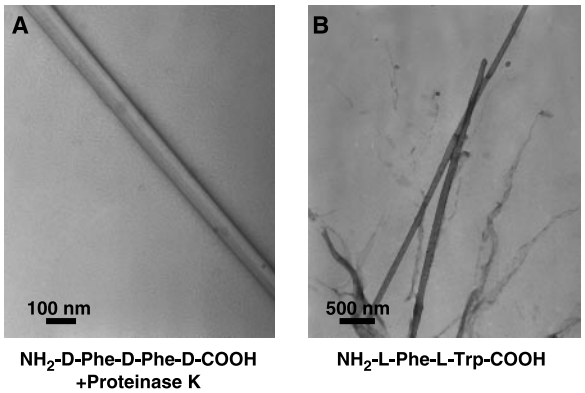

Fig. 4. Formation of peptide nanotubes by different aromatic peptides. (**A**) TEM image of the stable nanotubes formed by the D–amino acid building-block analog (**B**) TEM image of a tubular structure formed by the NH_2-Phe-Trp-COOH dipeptide. Amorphous aggregates can be observed in the background.

References and Notes

1. D. T. Bong, T. D. Clark, J. R. Granja, M. R. Ghadiri, *Angew. Chem. Int. Ed.* **40**, 988 (2001).
2. M. R. Ghadiri, J. R. Granja, R. A. Milligan, D. E. McRee, N. Khazanovich, *Nature* **366**, 324 (1993).
3. S. Vauthey, S. Santoso, H. Gong, N. Watson, S. Zhang, *Proc. Natl. Acad. Sci. U.S.A.* **99**, 5355 (2002).
4. S. Zhang, D. M. Marini, W. Hwang, S. Santoso, *Curr. Opin. Chem. Biol.* **6**, 865 (2002).
5. J. D. Hartgerink, J. R. Granja, R. A. Milligan, M. R. Ghadiri, *J. Am. Chem. Soc.* **118**, 43 (1996).
6. H. Matsui, B. Gologan, *J. Phys. Chem. B* **104**, 3383 (2000).
7. R. Azriel, E. Gazit, *J. Biol. Chem.* **276**, 34156 (2001).
8. Y. Mazor, S. Gilead, I. Benhar, E. Gazit, *J. Mol. Biol.* **322**, 1013 (2002).
9. M. Reches, Y. Porat, E. Gazit, *J. Biol. Chem.* **277**, 35475 (2002).
10. J. D. Harper, P. T. Lansbury Jr., *Annu. Rev. Biochem.* **66**, 385 (1997).
11. M. Sunde, C. C. Blake, *Q. Rev. Biophys.* **31**, 1 (1998).
12. C. M. Dobson, *Trends Biochem. Sci.* **24**, 329 (1999).
13. E. Gazit, *Angew. Chem. Int. Ed. Engl.* **114**, 257 (2002).
14. _____, *Curr. Med. Chem.* **9**, 1724 (2002).
15. R. B. Wickner *et al.*, *J. Struct. Biol.* **130**, 310 (2000).
16. E. Gazit, *FASEB J.* **16**, 77 (2002).
17. M. L. Waters, *Curr. Opin. Chem. Biol.* **6**, 736 (2002).
18. A. S. Shetty, J. Zhang, J. S. Moore, *J. Am. Chem. Soc.* **118**, 1019 (1996).
19. C. G. Claessens, J. F. Stoddart, *J. Phys. Org. Chem.* **10**, 254 (1997).
20. L. O. Tjernberg *et al.*, *J. Biol. Chem.* **271**, 8545 (1996).
21. M. A. Findeis *et al.*, *Biochemistry* **38**, 6791 (1999).
22. C. Soto *et al.*, *Nature Med.* **4**, 822 (1998).
23. M. A. Findeis, *Curr. Top. Med. Chem.* **2**, 417 (2002).
24. M. S. Wolfe, *Nature Rev. Drug. Discov.* **1**, 859 (2002).
25. C. H. Gorbitz, *Chemistry* **7**, 5153 (2001).
26. P. I. Haris, D. Chapman, *Biopolymers* **37**, 251 (1995).
27. M. F. Perutz, J. T. Finch, J. Berriman, A. Lesk, *Proc. Natl. Acad. Sci. U.S.A.* **99**, 5591 (2002).
28. A. Henglein, M. Giersig, *J. Phys. Chem. B.* **103**, 9533 (1999).
29. B. Enustun, J. Turkevich, *J. Am. Chem. Soc.* **85**, 3317 (1963).

30. Support from the Tel Aviv University Research Institute for Nanoscience and Nanotechnology Project and a Dan David Scholarship Award (to E.G.) are gratefully acknowledged. We thank A. Ulus for help with the SEM sample preparation and analysis, Y. Lereah and H. Moscovich for help in EDX analysis, Y. Delarea for help with TEM, and members of the Gazit laboratory for helpful discussions.

Supporting Online Material

www.sciencemag.org/cgi/content/full/300/5619/625/DC1

Materials and Methods

Figs. S1 to S4

15 January 2003; accepted 14 March 2003